PCCP

ROYAL SOCIETY OF CHEMISTRY

PERSPECTIVE

View Article Online
View Journal

Cite this: DOI: 10.1039/d5cp00604j

X-ray spectroscopy meets native mass spectrometry: probing gas-phase protein complexes†

Jocky C. K. Kung, ‡[abc] Alan Kádek, ‡[ade] Knut Kölbel,‡[f] Steffi Bandelow, [g] Sadia Bari, [hi] Jens Buck,[hj] Carl Caleman, [kl] Jan Commandeur,[m] Tomislav Damjanović,[abc] Simon Dörner,[af] Karim Fahmy, [n] Lara Flacht, [af] Johannes Heidemann,[f] Khon Huynh,[fo] Janine-Denise Kopicki,[ab] Boris Krichel,[ab] Julia Lockhauserbäumer,[f] Kristina Lorenzen,[e] Yinfei Lu,[f] Ronja Pogan,[ab] Jasmin Rehmann, [f] Kira Schamoni-Kast,[ab] Lucas Schwob, [h] Lutz Schweikhard, [g] Sebastian Springer,[p] Pamela H. W. Svensson, [k] Florian Simke, [g] Florian Trinter, [hq] Sven Toleikis, [h] Thomas Kierspel *[a] and Charlotte Uetrecht *[abc]

Gas-phase activation and dissociation studies of biomolecules, proteins and their non-covalent complexes using X-rays hold great promise for revealing new insights into the structure and function of biological samples. This is due to the unique properties of X-ray molecular interactions, such as site-specific and rapid ionization. In this perspective, we report and discuss the promise of first proof-of-principle studies of X-ray-induced dissociation of native (structurally preserved) biological samples ranging from small 17 kDa monomeric proteins up to large 808 kDa non-covalent protein assemblies conducted at a synchrotron (PETRA III) and a free-electron laser (FLASH2). A commercially available quadrupole time-of-flight mass spectrometer (Q-Tof Ultima US, Micromass/Waters), modified for high-mass analysis by MS Vision, was further adapted for integration with the open ports at the corresponding beamlines. The protein complexes were transferred natively into the gas phase *via* nano-electrospray ionization and subsequently probed by extreme ultraviolet (FLASH2) or soft X-ray (PETRA III) radiation, in either their folded state or following collision-induced activation in the gas phase. Depending on the size of the biomolecule and the activation method, protein fragmentation, dissociation, or enhanced ionization were observed. Additionally, an extension of the setup by ion mobility is described, which can serve as a powerful tool for structural separation of biomolecules prior to X-ray probing. The first experimental results are discussed in the broader context of current and upcoming X-ray sources, highlighting their potential for advancing structural biology in the future.

Received 14th February 2025,
Accepted 16th April 2025

DOI: 10.1039/d5cp00604j

rsc.li/pccp

[a] CSSB Centre for Structural Systems Biology, Deutsches Elektronen-Synchrotron DESY & Leibniz Institute of Virology (LIV) & University of Lübeck, Notkestraße 85, 22607 Hamburg, Germany. E-mail: thomas.kierspel@desy.de, charlotte.uetrecht@cssb-hamburg.de
[b] Institute of Chemistry and Metabolomics, University of Lübeck, Ratzeburger Allee 160, 23562 Lübeck, Germany
[c] Faculty V: School of Life Sciences, University of Siegen, Adolf-Reichwein-Str. 2a, 57076 Siegen, Germany
[d] Institute of Microbiology, Czech Academy of Sciences, Videnska 1083, 142 00 Prague, Czech Republic
[e] European XFEL, Holzkoppel 4, 22869 Schenefeld, Germany
[f] Leibniz Institute of Virology (LIV), Martinistraße 52, 20251 Hamburg, Germany
[g] Institute of Physics, University of Greifswald, Felix-Hausdorff-Str. 6, 17489 Greifswald, Germany
[h] Deutsches Elektronen-Synchrotron DESY, Notkestraße 85, 22607 Hamburg, Germany
[i] Zernike Institute for Advanced Materials, University of Groningen, Nijenborgh 3, 9747 AG Groningen, The Netherlands
[j] Institut für Experimentelle und Angewandte Physik, Christian-Albrechts-Universität zu Kiel, Leibnizstr. 19, 24118 Kiel, Germany
[k] Department of Physics and Astronomy, Uppsala University, Box 516, 75120 Uppsala, Sweden
[l] Center for Free-Electron Laser Science, Deutsches Elektronen-Synchrotron, 22607 Hamburg, Germany
[m] MS Vision, Televisieweg 40, 1322 AM Almere, The Netherlands
[n] Institute of Resource Ecology, Biophysics Division, Helmholtz-Zentrum Dresden-Rossendorf e.V. (HZDR), Bautzner Landstraße 400, 01328 Dresden, Germany
[o] School of Biomedical Engineering, International University, Vietnam National University, Ho Chi Minh City, Vietnam
[p] School of Science, Constructor University Bremen gGmbH, Research II-111, Campus Ring 1, 28759 Bremen, Germany
[q] Molecular Physics, Fritz-Haber-Institut der Max-Planck-Gesellschaft, Faradayweg 4-6, 14195 Berlin, Germany

† Electronic supplementary information (ESI) available. See DOI: https://doi.org/10.1039/d5cp00604j

‡ These authors contributed equally to this work.

Introduction

Electrospray ionization (ESI) of proteins and their complexes in combination with mass spectrometry (MS) is nowadays a standard technique in biophysics and structural biology due to its ease of application and its versatility of experiments. MS has been particularly successful in probing two fundamental aspects of proteins: their (amino acid) sequence and higher order structure.

Structural analysis, particularly the secondary to quaternary order conformation of biomolecules, has been largely enabled by advances in native MS,[1] which gently transfers proteins and their complexes from native-like aqueous solutions into the gas phase under close to native conditions (usually by nano-ESI[2]). This has been proven numerous times indirectly with ion mobility (IM) measurements,[3] free-electron laser (FEL) spectroscopy,[4] and through direct observation of single molecules *via* electron microscopy imaging subsequent to soft-landing of natively sprayed proteins.[5]

Tandem MS, where precursor ions are isolated by their mass-to-charge ratio (m/z) and subjected to fragmentation, followed by product ion identification, is extremely powerful for both, sequence and structure analysis. Laboratory-based fragmentation methods include collision-induced dissociation (CID), electron-based dissociation (ExD),[6] surface-induced dissociation (SID),[7] infrared multiphoton dissociation (IRMPD), and ultraviolet photodissociation (UVPD).[8,9] Each method of fragmentation has its own strengths and weaknesses. For example, CID involves slow heating through background gas collisions and intramolecular vibrational redistribution (IVR), potentially causing conformational changes before actual fragmentation. It is therefore of limited value to gaining higher order conformational information, but remains a powerful sequencing method. UVPD, on the other hand, is a faster fragmentation method and can therefore be more sensitive to the initial conformation of the samples.[10]

X-ray-induced fragmentation is considered an even faster, and hence structure-sensitive method. This rapid ionization and energy deposition result from the absorption of a single X-ray photon, followed by an ultrafast Auger–Meitner decay ($\sim$fs). Studies of the physical process of the excitation of biomolecules by X-rays, such as peptides and proteins, have been conducted previously.[11–14] The relaxation mechanism and the fragmentation pathways depend heavily on the size of the molecule. For small molecules, ejection of hydrogens or protons and small fragments are dominant. For smaller peptides, core-electron photoionization and subsequent relaxation processes (both the emission of photoelectrons and Auger–Meitner electrons) are followed by fragmentation pathways that produce small m/z fragments.[11] In larger proteins, after ionization, IVR can outcompete the fragmentation pathways, reducing the number of fragments produced after ionization. Besides, there is also the potential advantage of site-specific (localized) ionization. For example, element specificity or chemical environments, such as carbon 1s $\rightarrow$ π^*(C=C) excitations result in spectral features,[14] which can be connected to the conformation of the protein.

Using X-rays for the study of protein complexes may provide unique and complementary information that is not present in other structural-biology techniques. However, the interaction of large gaseous protein complexes, made feasible by native MS, with X-rays is not yet well understood. In order to take advantage of the rapid rate of relaxation by fragmentation as a tool to study the conformation of large biomolecules, it is necessary to understand the underlying physics of the process.

X-ray fragmentation may also be a complementary technique in (native) top-down (TD) MS. In TDMS, intact proteins and complexes are introduced into the mass spectrometer and subsequently fragmented to obtain structural information that spans from the protein sequence to subunit interactions in a complex.[15,16] The fast rate and rapid, localized energy deposition after the absorption of an X-ray photon is of particular interest in TDMS, as X-ray photodissociation may become a complementary method for improved protein sequence coverage and survival of post-translational modifications. In addition, X-ray fragmentation can be combined with other established gas-phase techniques such as ion-mobility spectrometry (IMS). In combination with simulations, IM-tandem MS can be a powerful tool for structural analysis of protein complexes.[17,18]

Furthermore, native MS can be used to study radiation damage in biomolecules in the gas phase, focusing on secondary ionization events from photo- and Auger–Meitner electrons—similar to those occurring in X-ray radiation-induced damage to biological tissues.[19] A better understanding of the effects of X-rays on biomolecules, including proteins, is crucial in the biomedical field. In this isolated gas-phase environment, native MS enables the study of X-ray effects on proteins without interference from environmental and surrounding factors.

Here, we present the first proof-of-principle experiments of our campaign to study the interaction of X-rays with gaseous proteins and their non-covalent complexes of various sizes obtained by native MS.

For our experiments, a commercially available high-mass Q-ToF mass spectrometer further modified for X-ray experiments was installed at multiple open-port beamlines at DESY in Hamburg, Germany. We focus on data collected from two beamlines, the synchrotron beamline P04 at PETRA III,[20] as well as the FL24 beamline of the free-electron laser FLASH2.[21] The experimental MS setup is capable of measuring proteins and protein complexes ranging from small peptides up to MDa virus-like particles (VLPs) with a diameter of more than $\sim$30–40 nm.[22–24] A quadrupole mass filter (QMF) was used to select molecular ions of a specific m/z in the gas phase before the X-ray interaction region. In addition, we demonstrate the use of CID and IM prior to probing the proteins by X-rays for pre-activation and conformational separation, respectively. The presented results are discussed in the context of future potential experiments and their current limitations.

Instrumental setup and experimental methods

Fig. 1 shows a schematic drawing of an X-ray coupled version of the quadrupole time-of-flight (Q-Tof Ultima US, Micromass/MS Vision)

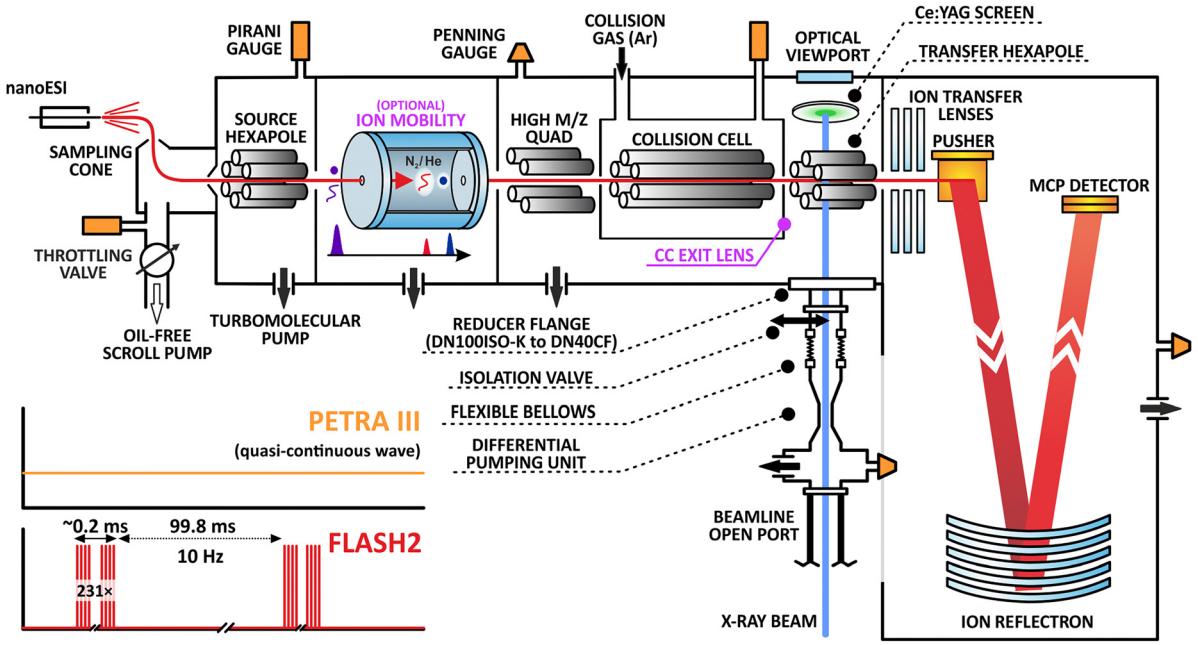

Fig. 1 Schematic of the experimental setup. Ions are generated from solution in a nano-ESI source and transported into the gas phase of a high-mass modified Q-ToF mass spectrometer to a microchannel plate (MCP) detector. As they fly past, they intersect perpendicularly with X-ray/EUV photons in a radially confining hexapole between the collision cell and the ToF analyzer. An optical viewport and a Ce:YAG screen were used to aid the alignment of the setup with respect to the photon beam. Magenta labels show the optional ion mobility device used for conformational separation and the collision cell (CC) exit lens used to temporarily trap ions as described in the main text. The inset illustrates the photon delivery structure of both the quasi-continuous PETRA III synchrotron (equally distributed pulses with 16 ns or 192 ns bunch spacing when operated at 62.5 MHz and 5.2 MHz, respectively) and the unevenly pulsed FLASH2 free-electron laser used for the reported experiments.

spectrometer modified for high mass.[25] Modifications beyond high-m/z capability include open-port access *via* a DN40 ConFlat (CF) vacuum flange at the transfer hexapole ion guide behind the collision cell for coupling to P04[20] at the PETRA III synchrotron or FL24 at the FLASH2 FEL.[26,27] The full details of the modifications for optical access are described in the ESI.†

For the experimental sequence, samples are transferred into the gas phase using ESI or nano-ESI. All protein and peptide samples or other materials are described in the ESI.† Experiments were performed in positive ion mode. Hence, ESI produces positively charged protein ions that enter the instrument. Afterwards, the ions were selected based on their m/z using the QMF of the Q-ToF. Depending on the pressure in, and the voltage gradient across the collision cell, samples were either merely thermalized and transported through the collision cell, which is aided by gentle collisional cooling and beam focusing, or vibrationally activated in the gas phase *via* energetic collisions with argon, before they were transported to the transfer hexapole ion guide and probed perpendicularly by the X-rays. The X-ray beam was typically much smaller in diameter—at most one tenth the size of the ion beam—allowing only a few percent of the direct ion beam to be probed by the X-rays. Ions (including the products) were then transferred to the pusher region, mass analyzed in the ToF region, and detected upon hitting a microchannel plate. Additional instrument components and measurement steps for pulsed operation were required at FLASH2 due to the long time period between the photon bunches, see the ESI† for further details.

For the ion-mobility X-ray experiments only, an additional vacuum chamber containing a resistive glass drift tube was installed in front of the source hexapole of the Q-ToF. The instrument components were obtained from MS Vision and the design is based on the MoQToF instrument by Barran and co-workers.[28,29]

Results and discussion

Fragmentation

Protein complex fragmentation experiments were performed at two different X-ray light sources, each corresponding to a distinct ionization regime. At the P04 beamline of PETRA III, protein complexes were probed *via* single-photon 1s core ionization at a photon energy of 595 eV using a pink (polychromatic) beam. In contrast, at the FL24 beamline of FLASH2, protein samples were probed *via* multiphoton inner-shell ionization at a photon energy of 163 eV and a pulse energy of 140 μJ, with a focus diameter (full width at half maximum) of 100 μm. Here, the absolute number of absorbed photons is difficult to estimate due to the complexity of the underlying ionization processes. For example, in the case of haemoglobin (Hb, Fig. 2d), these FEL parameters suggest the absorption of up to a couple hundred photons per FEL pulse. This estimate is based on the independent atom model, and neglects, *e.g.*, changes in absorption cross section due to the molecular orbitals or the increased ionization of the protein complex. Further, each photoelectron creates up to seven secondary

electrons, due to electron-impact ionization, within a volume with a radius of around 2.5 nm.[30] The resulting number suggests a very high state of ionization.

Fig. 2 shows a selection of protein complex mass spectra recorded with the instrumental setup at the two facilities. The spectra compare the protein complexes in the presence (on, coloured) and absence (off, black) of X-ray irradiation. Spectra in Fig. 2a–c were measured at the P04 beamline (yellow), the spectra in Fig. 2d were measured at the FLASH2 facility (blue). In Fig. 2a and b, spectra of non-preactivated, native-like protein complexes, bacterial chaperone GroEL (≈808 kDa, 14-mer) and disulfide-stabilized human leukocyte antigen (ds-HLA, ≈44 kDa, heterodimer comprising α_{1-3} heavy chain and β_2-microglobulin), are shown.[31] In contrast, Fig. 2c and d depict spectra of collisionally pre-activated ds-HLA and human haemoglobin (Hb, ≈64 kDa, heterotetramer comprising two α and two β subunits with or without a haem cofactor – holo-/apo-, respectively), *i.e.,* non-native and partially fragmented protein complexes. Labelled peaks denote identified dissociation products and their charge states.

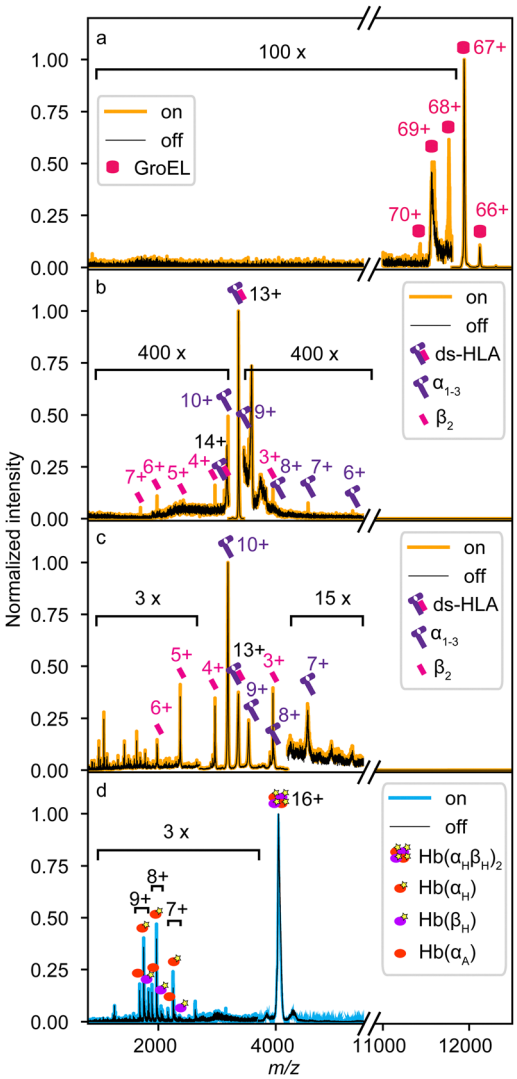

Fig. 2 Mass spectra of protein complexes in the presence (on, yellow or blue) and absence (off, black) of X-ray excitation. Spectra in panels (a)–(c) were measured at the PETRA III P04 beamline. Spectra in panel a show non-collisionally activated GroEL. In panels (b) and (c), mass spectra of non-collisionally activated and collisionally activated disulfide-stabilized human leukocyte antigen (ds-HLA), respectively, are depicted. Spectra of collisionally activated tetrameric haemoglobin (Hb) in panel (d) were measured at the FL24 beamline of the FLASH2 FEL.

Generally, the measured X-ray-induced product mass spectra are dominated by the direct ion beam, which can be attributed to the previously mentioned mismatch in ion and X-ray beam diameters, and the low probability of X-ray interaction as the ions were irradiated on-the-flight without extended ion trapping. The collisionally pre-activated samples in Fig. 2c and d exhibit a significantly higher fragment ion yield, as indicated by the much lower magnification factors required to visualize the X-ray-induced fragmentation channels. This can be qualitatively attributed to the increased internal energy from collision pre-activation, which lowers the energy threshold for fragmentation. However, contributions from conformational-change-related secondary ionization cannot be excluded either.

Fig. 2a shows the quadrupole-filtered and non-activated (native-like folded) GroEL. In the 'X-ray off' spectrum (black), the precursor ions of the 67+ charge state dominate the spectrum. Small amounts of 66+ and 69+ ions are present due to charge stripping of the complex accompanied by additional desolvation required after isolation in the QMF and/or incomplete mass filtering by the QMF itself. However, their relative intensity is below 1% compared to 67+ and negligible for the X-ray interaction. Upon X-ray irradiation, the 67+ charge state of the very large oligomer did not fragment, but multiple ionization events occurred, indicated by the 68+, 69+, and 70+ ions that are formed in the "X-ray on" spectrum (yellow). The ionization products can be explained by the emission of photoelectron and then subsequent Auger–Meitner electron(s) from the precursor complex as the excitation relaxation mechanisms. The lack of fragmentation is attributed to the size of GroEL, as larger complexes have more vibrational degrees of freedom to absorb the remaining energy after electron emissions, which is in line with studies conducted by Schlathölter and co-workers.[11]

Fig. 2b shows a similar initial situation for the non-activated heterodimer ds-HLA. The 13+ charge state is quadrupole-filtered and dominates the spectrum. In contrast to GroEL, the protein complex also shows a relatively minor peak for secondary ionization to 14+ but in addition primarily undergoes fragmentation into its α_{1-3} and β_2 subunits, similar to the products in an SID experiment.[32] The summed final charge states of the products can be estimated based on the relative peak intensities of the product ion peaks, which match ions with 13+, 14+, and 15+ charge states.

In the case of quadrupole-filtered and collisionally pre-activated ds-HLA (Fig. 2c), the situation is more complex. The spectrum is dominated by the α_{1-3} 10+ charge state, a fragment generated during the CID process. The initial quadrupole-filtered 13+ charge state has an intensity comparable to that of other ions produced through CID fragmentation. Thus, the X-rays probe multiple species at once. A general increase of the already populated fragmentation channels is visible, and new

fragmentation channels could be hidden in the significantly increased ion background due to the CID process. However, the ion signal of the β_2 3+, 4+, 5+, and 6+ subunits are clearly enhanced upon X-ray interaction, suggesting an origin in the heterodimeric ds-HLA 13+ precursor, as these β_2-subunits cannot come from the most abundant α_{1-3} 10+ ions. This pattern resembles that in Fig. 2b but occurs with significantly higher fragmentation efficiency. It can be explained by the increased internal energy of the protein complex due to the collisional activation prior to X-ray exposure.

Fig. 2d shows mass spectra of collisionally activated and quadrupole-filtered Hb 16+ proteins. In contrast to Fig. 2c, the CID spectrum is dominated by the precursor. CID fragments include both holo- (haem bound) and apo- (without haem) forms of monomers of both subunits, with intensities ranging from 1% to 20% of the main peak. Similar to Fig. 2c, the ionization due to the FEL primarily enhances existing CID fragmentation channels at a comparable high yield, albeit with slightly different branching ratios. This similarity suggests that the detected fragments from FEL ionization primarily originated from protein complexes that were probed at the edge of the FEL focus and ionized by only a few XUV photons. As mentioned above, for Hb, we estimate the absorption of a couple hundred photons in the focus of the FEL by the complex. Apparently, the chosen experimental setup is not optimal for this type of FEL experiment. The high number of absorbed photons likely induce a strong Coulomb explosion of the protein, generating small ionic fragments that are too fast to be retained and effectively transferred by the transfer hexapole with confining radio frequencies primarily optimized for larger species. This, together with the geometric distance between the interaction zone and the ToF analyzer's entrance, along with the ion spectrometer's lower detection limit of 150 m/z due to overwhelming electronic signal from the pusher, prevents the detection of these fragments.

Addition of mobility separation

Gas-phase structural techniques, such as IMS, are well established and can significantly enhance X-ray protein studies. By either analyzing or separating conformers, these techniques offer additional information beyond what is obtainable from MS alone and can therefore supplement X-ray fragmentation too. Furthermore, when combined with simulations, the measured collision cross sections offer new insights for the interpretation of the resulting fragments.

Fig. 3 shows the first proof-of-principle results from ion mobility experiments conducted with X-rays using synchrotron radiation. To enable these measurements, a custom-built drift tube[33] was installed on the Q-Tof Ultima US as shown in Fig. 3. The sample was a helix-turn-helix peptide (HTH, see ESI† for the sequence), similar to a study by Jarrold and co-workers.[34] The oligopeptide sample was first mobility-separated, then the doubly charged HTH peak at m/z 1321 was mass-selected before being probed by the X-rays.

As seen in the spectrum in Fig. 3 and indicated by the magnification factor, the filtering was less effective than in

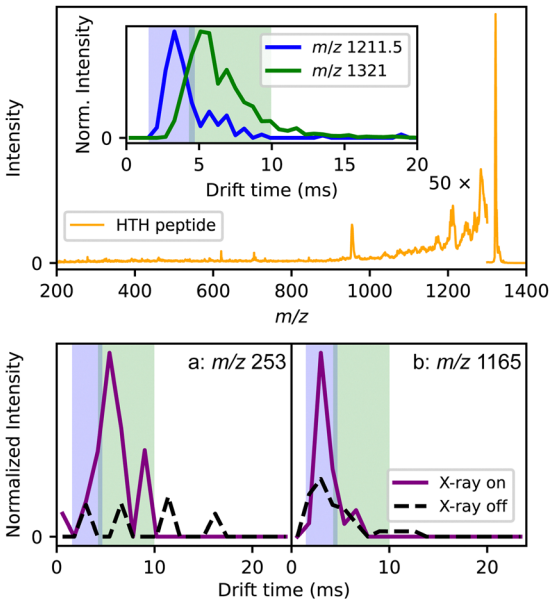

Fig. 3 Single-photon X-ray excitation of the helix-turn-helix peptide (HTH) sample. The upper panel contains the mass spectrum of the peptide after irradiation. The inset shows the arrival time distributions of the m/z representing HTH (m/z 1321) and the second most prominent peak in the mass spectrum from the sample (m/z 1211.5). The lower panel contains arrival time distributions of two fragment ions with and without irradiation.

Fig. 2, resulting in a very low signal-to-noise ratio for this experiment. However, the ion drift time could be used to discriminate between different species. According to the mass spectrum, the peptide sample contained multiple shorter peptides resulting from incomplete synthesis. In the top panel of Fig. 3, 1321 is the expected m/z of the HTH peptide while 1211.5 corresponds to the m/z of the peptide fragment lacking the last two residues. Their arrival time distributions are shown in the inset. Their drift times are different enough that fragments produced after irradiation from either the full peptide or the impurity can be distinguished; the ion-mobility separation is performed before the Q-ToF analysis and before fragmentation. In the bottom panel, the arrival time distributions of two potential fragment ions with m/z 253 and 1165 with and without X-ray excitation are depicted. The blue and green shaded areas mark the arrival time peaks of the full and partial peptide of the inset in the top panel, respectively.

The IM module is being further optimized, including the resolution of the measurements. Nonetheless, the distributions show the ability of distinguishing fragment ions as either being from the peptide or from impurities. As the instrument is optimized, selection of specific protein conformers before fragmentation will be feasible. This will allow the differentiation of fragmentation pathways of multiple conformers, and provide structural and sequence information as reported from other IMS combined with photodissociation techniques.[35–37]

Summary and outlook

In these first experiments of the X-ray excitation of gaseous protein and protein complex ions, we have demonstrated the

utility of native MS as a delivery system for X-ray excitation of isolated proteins, especially larger complexes in the range of 50 kDa to 1 MDa. The fragmentation pattern and pathway after irradiation are similar to the trend shown in previous studies of peptides and smaller proteins, with additional pathways that are not possible for monomeric proteins. In the presence of only X-ray irradiation, smaller protein complexes proceed in dissociation by breaking off non-covalent interactions after induced ionization, resulting in formation of protein subunits and ligands. For very large complexes, ionization by simple electron ejection and subsequent Auger–Meitner decay dominate. The fragment abundance from solely X-ray excitation is lower than in CID, although this is possibly due to low interaction probability of photons with complexes. In the present examples, X-ray excitation of already collisionally activated complexes generally enhances the CID fragmentation channels. These observations are in line with the model of vibration redistribution of energy after ejection of electrons,[11] in which larger protein complexes have more vibrational modes to distribute this energy, unless these are already diminished by collisional pre-activation. The addition of IMS before X-ray fragmentation is feasible and can be incorporated in the future for the study of large protein complexes.

From these initial experiments, we have recognized some limitations of the current instrumental setup and method. The major issue is the low signal-to-noise ratio. To increase this, we identified the background ion signal (as opposed to the analyte's intensity) as problematic with collisional pre-activation. That being said, the employment of sufficient mass filtering with no ion pre-activation results in very low ion background, allowing high sensitivity for the low-abundance products. Such an approach is suited when the subject of interest is in fragmentation mechanisms, specifically in irradiation-induced ionization of non-covalent complexes. Thus, even with the current background, native MS X-ray experiments are useful for spectroscopic and radiation damage studies.

For the increase in signal of the fragment ions, the issue is either low statistical probability of ion-photon interactions, or the difficulty in detecting product ions with high kinetic energy. As a side note, we saw high dissociation yields during one of the campaigns, suggesting that higher efficiency could be achieved (Fig. S1, ESI†). Thus, improvement of the instrumental setup illustrated in Fig. 1 must be considered. We note that the photons are transmitted between the rods of the last transfer-hexapole in front of the ToF analyzer, and ions are irradiated perpendicularly, 10 cm before they enter the ion transfer lens and pusher region of the spectrometer. The location was already chosen (mechanically) as close as possible to the entrance to the ToF region. It is unclear how many ions are lost in the hexapole after X-ray interaction due to high kinetic energies obtained during the relaxation process. This concern is especially important for experiments at FEL beamlines (Fig. 2d), where strong Coulomb explosions are expected. As such, FEL (or multiphoton) experiments would profit from an interaction point in the pusher region to extract the fragments as it could for instance be realized in the MS SPIDOC setup,[29] or from a gas-filled ion trap for cooling and trapping of fragments.[11,38,39]

Another possibility to consider is that the number of interaction events between the photons and complexes was low. If the absorption cross section is high, and yet for example, the X-ray-ion beam overlap is low, then absorption rarely takes place. This can be improved by irradiation in parts of the instrument where the ions are in higher density, such as in an ion trap, or by instrumentation that allows co-axial ion and photon beams for interaction.[40–42]

Finally, in order for the fragmentation to proceed, the fragmentation after absorption of the X-ray photon is due to energy left behind by the ionization/decay processes. In larger protein complexes, the reabsorption of any photoelectrons or Auger–Meitner electrons and subsequent ionization are expected to be substantial.[43] Therefore, the energy of the ejected electron from the core is an important parameter to investigate. This can be measured by tuning the photon energy and conducting spectroscopy experiments to gain a deeper understanding of the relaxation pathways of proteins of different sizes, following X-ray photon absorption at different energies, which is a unique feature available for these wavelengths exclusively at synchrotrons and FELs.[13]

In comparison to other MS fragmentation techniques,[15] such as ExD or UVPD, not as many different pathways of fragmentation have appeared after X-ray irradiation. Two main strategies can be employed to use X-rays as a complementary technique for TDMS and spectroscopic experiments. The first approach involves investigating changes in X-ray photon energy, as mentioned above. The second involves MS^n experiments, where various activation methods (including X-rays) are combined with additional filtering of individual species after CID or X-ray interaction. This could be achieved, for instance, using an Omnitrap platform,[44] which is particularly well-suited for cycling and filtering reaction products.

In terms of the future for employing native MS as a sample delivery system for X-ray experiments, the delivery of natively folded, mass and conformationally selected protein complexes is mature for fragmentation experiments, and moreover a wide variety of other X-ray experiments of large biomolecules. The MS SPIDOC project was conceived to leverage the techniques known in mass spectrometry for background-free, highly selective single-particle imaging.[29,33]

The absorption of large numbers of photons, which might have been a concern for a fragmentation experiment inside a modified commercial instrument, can become an advantage for ion imaging experiments such as velocity map imaging (VMI) or Coulomb explosion imaging of biological structures.[45,46]

Moreover, since experiments are often conducted at large light source facilities, additional lasers are available for pump–probe experiments. This enhances the potential of using native MS as a promising sample delivery method for studying structural changes in biomolecules in real time. Recent work highlights the capability of native MS to look at complex kinetics in proteins and protein complexes.[47–50]

With our initial experiments and studies, the combination of native MS and X-ray sources promises to become an invaluable tool in structural biology, biophysics, and spectroscopy.

Author contributions

Conceptualization – A. K., K. K., J. C., T. K., C. U. Methodology – J. C. K. K., A. K., K. K., St. B., J. C., T. D., Y. L., T. K., C. U. Software – J. C. K. K., T. D., S. D., Y. L., F. S., T. K. validation – J. C. K. K., A. K., K. K., Y. L., T. K. formal analysis – J. C. K. K., A. K., K. K., Y. L., T. K. investigation – J. C. K. K., A. K., K. K., St. B., Sa. B., J. B., J. C., T. D., S. D., L. F., J. H., K. H., J.-D. K., B. K., J. L., Y. L., R. P., J. R., K. S.-K., Lucas. S., P. H. W. S., F. S., F. T., S. T., T. K., C. U. Resources – J. B., J. C., K. F., K. L., Lutz S., S. S., F. T., S. T., C. U. Data curation – K. K., T. D., Y. L., T. K. writing – original draft – J. C. K. K., A. K., T. K. writing – review & editing – K. K., St. B., Sa. B., J. B., C. C., S. D., L. F., J. H., K. H., J.-D. K., B. K., J. L., Y. L., R. P., J. R., K. S.-K., Lucas. S., Lutz S., S. S., P. H. W. S., F. S., F. T., S. T., C. U. Visualization – J. C. K. K., A. K., K. K., T. K. supervision – A. K., C. C., K. L., Lucas. S., Lutz S., T. K., C. U. Project administration – A. K., T. K., C. U. Funding acquisition – Sa. B., C. C., Lutz S., C. U.

Data availability

The data supporting this study, along with scripts for data analysis, are available at the following link: **https://syncandshare.desy.de/index.php/s/RSqsMgpL9PoWn2A**.

Conflicts of interest

There are no conflicts to declare.

Acknowledgements

We would like to thank everyone that has been involved in this experimental campaign. We acknowledge DESY (Hamburg, Germany), a member of the Helmholtz Association HGF, for the provision of experimental facilities. Parts of this research were carried out at FLASH and PETRA III. We would like to thank Moritz Hoesch and Marion Kuhlmann for assistance in using P04 and FL24, respectively. Beamtimes were allocated for proposals F-20150009, F-20171103, I-20180927, I-20190534, and I-20221192. We also acknowledge members of the MS SPIDOC consortium, the Uetrecht group (Hao Yan) and collaborators, including at the Universität Greifswald (Paul Fischer, Gerrit Marx), the University of Hamburg (Henning Tidow), European XFEL (Joachim Schulz, Carsten Deiter, James Moore, Rita Graceffa, Matthäus Kitel) for their participation in the beamline experiments. Finally, we acknowledge all the funding agencies that made this project possible: J. C. K. K., A. K., St. B., C. C., J. C., T. D., K. H., K. L., Y. L., L.utz S., F. S., T. K., and C. U. acknowledge the funding of MS SPIDOC by the European Union's Horizon 2020 research and innovation program (grant agreement no. 801406). K. S.-K., K. K., and C. U. acknowledge the funding of ERC SPOCk'S MS by the ERC (grant agreement no. 759661). C. U. acknowledges the funding of PIER Ideenfonds from DESY and the University of Hamburg. Leibniz Institute for Experimental Virology is supported by the Free and Hanseatic City of Hamburg and the German Federal Ministry of Health. J. C. K. K., C. C., T. D., and C. U. acknowledge support from a Röntgen Ångström Cluster grant provided by the Swedish Research Council and the Bundesministerium für Bildung und Forschung (2021-05988, 05K22PSA). A. K. gratefully acknowledges an Alexander von Humboldt postdoctoral fellowship (1196583-HFST-P). C. U., A. K., and Lutz S. further acknowledge funding through Bundesministerium für Bildung und Forschung (BMBF) 05K2016 VISAVIX (05K16HG1, 05K16BH1). Sa. B. and Lucas S. acknowledge funding by the Helmholtz Initiative and Networking Fund and Sa. B. acknowledges further support by the Cluster of Excellence 'CUI: Advanced Imaging of Matter' of the Deutsche Forschungsgemeinschaft (DFG) – EXC 2056 – project ID 390715994. C. C. and P. H. W. S. acknowledge support from the Swedish Research Council through projects 2021-05988 and 2018-00740. C. C. acknowledges support from the Helmholtz Association through the Center for Free-Electron Laser Science at DESY. S. D. and C. U. acknowledge funding from VirMScan, provided by the Bundesministerium für Bildung und Forschung (BMBF 13GW0622). L. F. was funded by the Promotion of young CSSB scientists' program by the Joachim Herz Foundation. F. T. acknowledges funding by the Deutsche Forschungsgemeinschaft (DFG, German Research Foundation) – Project 509471550, Emmy Noether Programme.

References

1 A. C. Leney and A. J. R. Heck, Native Mass Spectrometry: What is in the Name?, *J. Am. Soc. Mass Spectrom.*, 2017, **28**, 5–13.
2 M. Karas, U. Bahr and T. Dülcks, Nano-electrospray ionization mass spectrometry: addressing analytical problems beyond routine, *Fresenius' J. Anal. Chem.*, 2000, **366**, 669–676.
3 C. Lapthorn, F. Pullen and B. Z. Chowdhry, Ion mobility spectrometry-mass spectrometry (IMS-MS) of small molecules: Separating and assigning structures to ions, *Mass Spectrom. Rev.*, 2013, **32**, 43–71.
4 J. Seo, W. Hoffmann, S. Warnke, M. T. Bowers, K. Pagel and G. von Helden, Retention of Native Protein Structures in the Absence of Solvent: A Coupled Ion Mobility and Spectroscopic Study, *Angew. Chem., Int. Ed.*, 2016, **55**, 14173–14176.
5 T. K. Esser, J. Böhning, A. Önür, D. K. Chinthapalli, L. Eriksson, M. Grabarics, P. Fremdling, A. Konijnenberg, A. Makarov, A. Botman, C. Peter, J. L. P. Benesch, C. V. Robinson, J. Gault, L. Baker, T. A. M. Bharat and S. Rauschenbach, Cryo-EM of soft-landed β-galactosidase: Gas-phase and native structures are remarkably similar, *Sci. Adv.*, 2024, **10**, eadl4628.
6 K. O. Zhurov, L. Fornelli, M. D. Wodrich, Ü. A. Laskay and Y. O. Tsybin, Principles of electron capture and transfer dissociation mass spectrometry applied to peptide and protein structure analysis, *Chem. Soc. Rev.*, 2013, **42**, 5014–5030.
7 D. T. Snyder, S. R. Harvey and V. H. Wysocki, Surface-induced Dissociation Mass Spectrometry as a Structural Biology Tool, *Chem. Rev.*, 2022, **122**, 7442–7487.
8 P. Maitre, D. Scuderi, D. Corinti, B. Chiavarino, M. E. Crestoni and S. Fornarini, Applications of Infrared

Multiple Photon Dissociation (IRMPD) to the Detection of Posttranslational Modifications, *Chem. Rev.*, 2020, **120**, 3261–3295.

9 J. S. Brodbelt, L. J. Morrison and I. Santos, Ultraviolet Photodissociation Mass Spectrometry for Analysis of Biological Molecules, *Chem. Rev.*, 2020, **120**, 3328–3380.

10 S. A. McLuckey and D. E. Goeringer, Slow Heating Methods in Tandem Mass Spectrometry, *J. Mass Spectrom.*, 1997, **32**, 461–474.

11 D. Egorov, L. Schwob, M. Lalande, R. Hoekstra and T. Schlathölter, Near edge X-ray absorption mass spectrometry of gas phase proteins: the influence of protein size, *Phys. Chem. Chem. Phys.*, 2016, **18**, 26213–26223.

12 D. Egorov, S. Bari, R. Boll, S. Dörner, S. Deinert, S. Techert, R. Hoekstra, V. Zamudio-Bayer, R. Lindblad, C. Bülow, M. Timm, B. von Issendorff, J. T. Lau and T. Schlathölter, Near-Edge Soft X-ray Absorption Mass Spectrometry of Protonated Melittin, *J. Am. Soc. Mass Spectrom.*, 2018, **29**, 2138–2151.

13 S. Bari, D. Egorov, T. L. C. Jansen, R. Boll, R. Hoekstra, S. Techert, V. Zamudio-Bayer, C. Bülow, R. Lindblad, G. Leistner, A. Ławicki, K. Hirsch, P. S. Miedema, B. von Issendorff, J. T. Lau and T. Schlathölter, Soft X-ray Spectroscopy as a Probe for Gas-Phase Protein Structure: Electron Impact Ionization from Within, *Chem. – Eur. J.*, 2018, **24**, 7631–7636.

14 S. Dörner, L. Schwob, K. Atak, K. Schubert, R. Boll, T. Schlathölter, M. Timm, C. Bülow, V. Zamudio-Bayer, B. von Issendorff, J. T. Lau, S. Techert and S. Bari, Probing Structural Information of Gas-Phase Peptides by Near-Edge X-ray Absorption Mass Spectrometry, *J. Am. Soc. Mass Spectrom.*, 2021, **32**, 670–684.

15 M. Zhou, C. Lantz, K. A. Brown, Y. Ge, L. Paša-Tolić, J. A. Loo and F. Lermyte, Higher-order structural characterisation of native proteins and complexes by top-down mass spectrometry, *Chem. Sci.*, 2020, **11**, 12918–12936.

16 R. Liu, S. Xia and H. Li, Native top-down mass spectrometry for higher-order structural characterization of proteins and complexes, *Mass Spectrom. Rev.*, 2023, **42**, 1876–1926.

17 C. Uetrecht, R. J. Rose, E. van Duijn, K. Lorenzen and A. J. R. Heck, Ion mobility mass spectrometry of proteins and protein assemblies, *Chem. Soc. Rev.*, 2010, **39**, 1633–1655.

18 E. G. Marklund, M. T. Degiacomi, C. V. Robinson, A. J. Baldwin and J. L. P. Benesch, Collision Cross Sections for Structural Proteomics, *Structure*, 2015, **23**, 791–799.

19 J. Narayanan S J, D. Tripathi, P. Verma, A. Adhikary and A. K. Dutta, Secondary Electron Attachment-Induced Radiation Damage to Genetic Materials, *ACS Omega*, 2023, **8**, 10669–10689.

20 J. Viefhaus, F. Scholz, S. Deinert, L. Glaser, M. Ilchen, J. Seltmann, P. Walter and F. Siewert, The Variable Polarization XUV Beamline P04 at PETRA III: Optics, mechanics and their performance, *Nucl. Instrum. Methods Phys. Res., Sect. A*, 2013, **710**, 151–154.

21 B. Faatz, M. Braune, O. Hensler, K. Honkavaara, R. Kammering, M. Kuhlmann, E. Ploenjes, J. Roensch-Schulenburg, E. Schneidmiller, S. Schreiber, K. Tiedtke, M. Tischer, R. Treusch, M. Vogt, W. Wurth, M. Yurkov and J. Zemella, The FLASH Facility: Advanced Options for FLASH2 and Future Perspectives, *Appl. Sci.*, 2017, **7**, 1114.

22 R. Pogan, V. U. Weiss, K. Bond, J. Dülfer, C. Krisp, N. Lyktey, J. Müller-Guhl, S. Zoratto, G. Allmaier, M. F. Jarrold, C. Muñoz-Fontela, H. Schlüter and C. Uetrecht, N-terminal VP1 Truncations Favor T = 1 Norovirus-Like Particles, *Vaccines*, 2021, **9**, 8.

23 R. Pogan, C. Schneider, R. Reimer, G. Hansman and C. Uetrecht, Norovirus-like VP1 particles exhibit isolate dependent stability profiles, *J. Phys.: Condens. Matter*, 2018, **30**, 064006.

24 C. Uetrecht, C. Versluis, N. R. Watts, W. H. Roos, G. J. L. Wuite, P. T. Wingfield, A. C. Steven and A. J. R. Heck, High-resolution mass spectrometry of viral assemblies: Molecular composition and stability of dimorphic hepatitis B virus capsids, *Proc. Natl. Acad. Sci. U. S. A.*, 2008, **105**, 9216–9220.

25 R. H. H. van den Heuvel, E. van Duijn, H. Mazon, S. A. Synowsky, K. Lorenzen, C. Versluis, S. J. J. Brouns, D. Langridge, J. van der Oost, J. Hoyes and A. J. R. Heck, Improving the Performance of a Quadrupole Time-of-Flight Instrument for Macromolecular Mass Spectrometry, *Anal. Chem.*, 2006, **78**, 7473–7483.

26 K. Tiedtke, A. Azima, N. von Bargen, L. Bittner, S. Bonfigt, S. Düsterer, B. Faatz, U. Frühling, M. Gensch, C. Gerth, N. Guerassimova, U. Hahn, T. Hans, M. Hesse, K. Honkavaar, U. Jastrow, P. Juranic, S. Kapitzki, B. Keitel, T. Kracht, M. Kuhlmann, W. B. Li, M. Martins, T. Núñez, E. Plönjes, H. Redlin, E. L. Saldin, E. A. Schneidmiller, J. R. Schneider, S. Schreiber, N. Stojanovic, F. Tavella, S. Toleikis, R. Treusch, H. Weigelt, M. Wellhöfer, H. Wabnitz, M. V. Yurkov and J. Feldhaus, The soft x-ray free-electron laser FLASH at DESY: beamlines, diagnostics and end-stations, *New J. Phys.*, 2009, **11**, 023029.

27 J. Rossbach, in *Synchrotron Light Sources and Free-Electron Lasers: Accelerator Physics, Instrumentation and Science Applications*, ed. E. J. Jaeschke, S. Khan, J. R. Schneider and J. B. Hastings, Springer International Publishing, Cham, 2016, pp. 303–328.

28 B. J. McCullough, J. Kalapothakis, H. Eastwood, P. Kemper, D. MacMillan, K. Taylor, J. Dorin and P. E. Barran, Development of an Ion Mobility Quadrupole Time of Flight Mass Spectrometer, *Anal. Chem.*, 2008, **80**, 6336–6344.

29 T. Kierspel, A. Kadek, P. Barran, B. Bellina, A. Bijedic, M. N. Brodmerkel, J. Commandeur, C. Caleman, T. Damjanović, I. Dawod, E. De Santis, A. Lekkas, K. Lorenzen, L. López Morillo, T. Mandl, E. G. Marklund, D. Papanastasiou, L. A. I. Ramakers, L. Schweikhard, F. Simke, A. Sinelnikova, A. Smyrnakis, N. Timneanu, C. Uetrecht and for the MS SPIDOC Consortium, Coherent diffractive imaging of proteins and viral capsids: simulating MS SPIDOC, *Anal. Bioanal. Chem.*, 2023, **415**, 4209–4220.

30 C. Caleman, C. Ortiz, E. Marklund, F. Bultmark, M. Gabrysch, F. G. Parak, J. Hajdu, M. Klintenberg and N. Tîmneanu, Radiation damage in biological material:

Electronic properties and electron impact ionization in urea, *Europhys. Lett.*, 2009, **85**, 18005.
31 J.-D. Kopicki, A. Saikia, S. Niebling, C. Günther, R. Anjanappa, M. Garcia-Alai, S. Springer and C. Uetrecht, Opening opportunities for Kd determination and screening of MHC peptide complexes, *Commun. Biol.*, 2022, **5**, 488.
32 R. L. Beardsley, C. M. Jones, A. S. Galhena and V. H. Wysocki, Noncovalent Protein Tetramers and Pentamers with ''n'' Charges Yield Monomers with n/4 and n/5 Charges, *Anal. Chem.*, 2009, **81**, 1347–1356.
33 A. Kadek, K. Lorenzen, C. Uetrecht and for the MS SPIDOC consortium, In a flash of light: X-ray free electron lasers meet native mass spectrometry, *Drug Discovery Today:Technol.*, 2021, **39**, 89–99.
34 D. T. Kaleta and M. F. Jarrold, Helix–Turn–Helix Motifs in Unsolvated Peptides, *J. Am. Chem. Soc.*, 2003, **125**, 7186–7187.
35 A. Theisen, B. Yan, J. M. Brown, M. Morris, B. Bellina and P. E. Barran, Use of Ultraviolet Photodissociation Coupled with Ion Mobility Mass Spectrometry To Determine Structure and Sequence from Drift Time Selected Peptides and Proteins, *Anal. Chem.*, 2016, **88**, 9964–9971.
36 F. C. Liu, M. E. Ridgeway, J. S. R. V. Winfred, N. C. Polfer, J. Lee, A. Theisen, C. A. Wootton, M. A. Park and C. Bleiholder, Tandem-trapped ion mobility spectrometry/mass spectrometry coupled with ultraviolet photodissociation, *Rapid Commun. Mass Spectrom.*, 2021, **35**, e9192.
37 M. Santos-Fernandez, K. Jeanne Dit Fouque and F. Fernandez-Lima, Integration of Trapped Ion Mobility Spectrometry and Ultraviolet Photodissociation in a Quadrupolar Ion Trap Mass Spectrometer, *Anal. Chem.*, 2023, **95**, 8417–8422.
38 S. Bari, O. Gonzalez-Magaña, G. Reitsma, J. Werner, S. Schippers, R. Hoekstra and T. Schlathölter, Photodissociation of protonated leucine-enkephalin in the VUV range of 8–40 eV, *J. Chem. Phys.*, 2011, **134**, 024314.
39 B. Bellina, J. M. Brown, J. Ujma, P. Murray, K. Giles, M. Morris, I. Compagnon and P. E. Barran, UV photodissociation of trapped ions following ion mobility separation in a Q-ToF mass spectrometer, *Analyst*, 2014, **139**, 6348–6351.
40 S. Warnke, C. Baldauf, M. T. Bowers, K. Pagel and G. von Helden, Photodissociation of Conformer-Selected Ubiquitin Ions Reveals Site-Specific Cis/Trans Isomerization of Proline Peptide Bonds, *J. Am. Chem. Soc.*, 2014, **136**, 10308–10314.
41 A.-L. Simon, F. Chirot, C. M. Choi, C. Clavier, M. Barbaire, J. Maurelli, X. Dagany, L. MacAleese and P. Dugourd, Tandem ion mobility spectrometry coupled to laser excitation, *Rev. Sci. Instrum.*, 2015, **86**, 094101.
42 S. Daly, L. MacAleese, P. Dugourd and F. Chirot, Combining Structural Probes in the Gas Phase – Ion Mobility-Resolved Action-FRET, *J. Am. Soc. Mass Spectrom.*, 2018, **29**, 133–139.
43 C. Caleman, G. Huldt, F. R. N. C. Maia, C. Ortiz, F. G. Parak, J. Hajdu, D. van der Spoel, H. N. Chapman and N. Timneanu, On the Feasibility of Nanocrystal Imaging Using Intense and Ultrashort X-ray Pulses, *ACS Nano*, 2011, **5**, 139–146.
44 D. Papanastasiou, D. Kounadis, A. Lekkas, I. Orfanopoulos, A. Mpozatzidis, A. Smyrnakis, E. Panagiotopoulos, M. Kosmopoulou, M. Reinhardt-Szyba, K. Fort, A. Makarov and R. A. Zubarev, The Omnitrap Platform: A Versatile Segmented Linear Ion Trap for Multidimensional Multiple-Stage Tandem Mass Spectrometry, *J. Am. Soc. Mass Spectrom.*, 2022, **33**, 1990–2007.
45 C. Östlin, N. Tîmneanu, H. O. Jönsson, T. Ekeberg, A. V. Martin and C. Caleman, Reproducibility of single protein explosions induced by X-ray lasers, *Phys. Chem. Chem. Phys.*, 2018, **20**, 12381–12389.
46 E. De Santis, I. Dawod, T. André, S. Cardoch, N. Timneanu and C. Caleman, Ultrafast X-ray laser-induced explosion: How the depth influences the direction of the ion trajectory, *Europhys. Lett.*, 2024, **148**, 17001.
47 J. Snijder, J. M. Schuller, A. Wiegard, P. Lössl, N. Schmelling, I. M. Axmann, J. M. Plitzko, F. Förster and A. J. R. Heck, Structures of the cyanobacterial circadian oscillator frozen in a fully assembled state, *Science*, 2017, **355**, 1181–1184.
48 L. Sänger, H. M. Williams, D. Yu, D. Vogel, J. Kosinski, M. Rosenthal and C. Uetrecht, RNA to Rule Them All: Critical Steps in Lassa Virus Ribonucleoparticle Assembly and Recruitment, *J. Am. Chem. Soc.*, 2023, **145**, 27958–27974.
49 R. Zangl, S. Soravia, M. Saft, J. G. Löffler, J. Schulte, C. J. Rosner, J. Bredenbeck, L.-O. Essen and N. Morgner, Time-Resolved Ion Mobility Mass Spectrometry to Solve Conformational Changes in a Cryptochrome, *J. Am. Chem. Soc.*, 2024, **146**, 14468–14478.
50 K. Schamoni-Kast, B. Krichel, T. Damjanović, T. Kierspel, S. Toker and C. Uetrecht, The kinetics of SARS-CoV-2 nsp7-11 polyprotein processing and impact on complexation with nsp16, *bioRxiv*, 2024, DOI: **10.1101/2024.01.06.574466**.